THE ROLE OF A STEEPNESS PARAMETER IN THE EXPONENTIAL STABILITY OF A MODEL PROBLEM. NUMERICAL ASPECTS

N. Todorović

Astronomical Observatory, Volgina 7, 11060 Belgrade 38, Serbia

E–mail: *ntodorovic@aob.rs*

SUMMARY: The Nekhoroshev theorem considers quasi integrable Hamiltonians providing stability of actions in exponentially long times. One of the hypothesis required by the theorem is a mathematical condition called steepness. Nekhoroshev conjectured that different steepness properties should imply numerically observable differences in the stability times. After a recent study on this problem (Guzzo et al. 2011, Todorović et al. 2011) we show some additional numerical results on the change of resonances and the diffusion laws produced by the increasing effect of steepness. The experiments are performed on a 4-dimensional steep symplectic map designed in a way that a parameter smoothly regulates the steepness properties in the model.

Key words. Celestial mechanics – Methods: numerical

1. INTRODUCTION

Providing effective stability estimates in the solar system has been an intriguing task since many years, decades and even centuries. Significant progress on this issue enabled the Hamiltonian perturbation theory with its two most outstanding theorems: KAM and the Nekhoroshev theorem which, under certain conditions, are able to provide stability in very long times. Good candidates in the solar system for the Nekhoroshev like stability are recognized in the neighborhood of the L_4 and L_5 stability points (Celletti and Giorgilli 1991, Efthymiopoulos 2005, Lhotka et al. 2008, Giorgilli and Skokos 1997) and in some regions of the asteroid belt (Pavlović and Guzzo 2008, Morbidelli and Guzzo 1997, Guzzo and Morbidelli 1996, Guzzo et al. 2002).

The Nekhoroshev theorem applies to analytic, slightly perturbed Hamiltonians whose integrable approximations are non degenerate functions satisfying a mathematical condition called *steepness*. We observe a model of a steep symplectic map (defined in

Guzzo et al. 2011) in order to show the influence of steepness on the resonant structure and the stability properties of actions. In addition to the perturbing parameter ε, the model also contains a parameter m that smoothly changes the steepness properties in the system. The goal of this research is to present a change of the diffusion laws caused by the increasing steepness effects in accordance with the Nekhoroshev theorem. The system is investigated numerically using methods developed in the last decade (Guzzo et al. 2002, Lega et al. 2003, Froeschlé et al. 2005). For five different values of the steepness parameter m, we observe the dependence between the diffusion coefficient D and the perturbation ε. The obtained results on diffusion confirm the expectations on the stabilizing steepness effects. Due to numerical limitations the nature of this change could not be properly estimated. In Todorović et al. (2011) this problem was observed from another aspect and it was shown that the relation between steepness and diffusion has an exponential character.

25

The paper is organized as follows: In Section 2 we introduce the Nekhoroshev theorem and the main definitions of steepness; the model studied in the paper is defined and explained in Section 3. The Arnold web of the model and its changes while changing the two parameters (m and ε) are described in Section 4. In Section 5 we give a short description of the resonant dynamics and the algorithm for the diffusion coefficient computation. Section 6 contains the numerical results about the influence of the parameter of steepness on the diffusion laws, while the final conclusions are given in Section 7.

2. THE NEKHOROSHEV THEOREM

One of the main results of the Nekhoroshev theorem considers stability estimates in quasi integrable Hamiltonians:

$$H(I, \varphi) = H_0(I) + \varepsilon H_1(I, \varphi) \qquad (1)$$

where $I \times \varphi \in \mathbb{D} \times \mathbb{T}^n$, $\mathbb{D} \subseteq \mathbb{R}^n$ are the action-angle variables, $H_0(I)$ is the integrable approximation and $H_1(I, \varphi)$ the perturbing function generated by a small parameter ε. In the case of zero perturbation ($\varepsilon = 0$), the system is integrable and reveals trivial motions: the actions are constant and the angular variables have constant frequencies. Already for small perturbations the integrability brakes down. The actions are not constant anymore, but they remain close to their initial values in finite times. The Nekhoroshev theorem provides a finer estimate of these changes and a deeper insight into the dynamical nature of Hamiltonian system (1).

The theorem states that if the Hamiltonian function H is analytic and the integrable approximation $H_0(I_1, .., I_n)$ is a non degenerate steep function, then there exists a critical ε_0, such that $\forall \varepsilon < \varepsilon_0$, every initial condition $(I, \varphi) \in \mathbb{D} \times \mathbb{T}^n$ is bounded with:

$$|I(t) - I(0)| < c\varepsilon^a \qquad (2)$$

in times such that

$$|t| < d \exp(\frac{\varepsilon_0}{\varepsilon})^b \qquad (3)$$

where a, b, c and d are some suitable positive constants which depend only on H_0.

The simplest examples of steep functions are given with *convex*, *quasi-convex* and *3-jet* functions. We say that a real analytic function h:

$$
\begin{aligned}
h : \mathbb{D} &\rightarrow \mathbb{R}^n \\
I &\rightarrow h(I)
\end{aligned}
$$

where $\mathbb{D} \subseteq \mathbb{R}^n$ is open and bounded and $\mathbf{u} \in \mathbb{R}^n$, is:

i) *Convex* at $I \in \mathbb{D}$ if the only real solutions of the equation:

$$\sum_{i,j=1}^n \frac{\partial^2 h}{\partial I_i \partial I_j}(I)u_i u_j = 0 \qquad (4)$$

is the trivial solution $\mathbf{u} = 0$.

ii) *Quasi-convex* at $I \in \mathbb{D}$ if the only real solution of the system:

$$
\begin{aligned}
\sum_{i=1}^n \frac{\partial h}{\partial I_i}(I)u_i &= 0 \\
\sum_{i,j=1}^n \frac{\partial^2 h}{\partial I_i \partial I_j}(I)u_i u_j &= 0
\end{aligned}
\qquad (5)
$$

is the trivial solution $\mathbf{u} = 0$.

iii) Satisfies the *3-jet* condition at $I \in \mathbb{D}$ if the only solution of the system

$$
\begin{aligned}
\sum_{i=1}^n \frac{\partial h}{\partial I_i}(I)u_i &= 0 \\
\sum_{i,j=1}^n \frac{\partial^2 h}{\partial I_i \partial I_j}(I)u_i u_j &= 0 \\
\sum_{i,j,k=1}^n \frac{\partial^3 h}{\partial I_i \partial I_j \partial I_k}(I)u_i u_j u_k &= 0
\end{aligned}
\qquad (6)
$$

is the trivial solution $\mathbf{u} = 0$.

The three listed cases are only *examples* of steep functions, while the exact definition of steepness is more implicit and can be found in Nekhoroshev (1977). It is expected that the most stable ones are the quasi-convex functions. This conjecture was numerically checked in Guzzo et al. (2011). It is also expected that besides the perturbation, steepness also plays a role in the dynamics. In terms of the exponential stability, it would mean that the exponent b in Eq. (3) increases as the system becomes steeper. Even though it is expected that these changes could be numerically confirmed, such an experiment is a very challenging task, since it considers changes in the slow Arnold diffusion, a phenomenon which is already difficult to observe.

The goal of this investigation is to verify, if possible, changes in stability times provoked by the increasing steepness effects. The experiments are done on a model defined by a 4-dimensional symplectic map in its non-convex steep (3-jet) domain.

3. THE MODEL PROBLEM

Symplectic maps are a very useful tool in Hamiltonian dynamics. In general, they present some kind of discrete Hamiltonian systems. Having the properties of the corresponding Hamiltonian and, at the same time, a relatively simple form, they allow a large spectrum of numerical investigations. The model we study (defined in Guzzo et al. 2011) is a 4-dimensional symplectic map ϕ :

$$
\begin{aligned}
\phi : \mathbb{R}^2 \times \mathbb{T}^2 &\rightarrow \mathbb{R}^2 \times \mathbb{T}^2, \\
(I_1, I_2, \varphi_1, \varphi_2) &\rightarrow (I'_1, I'_2, \varphi'_1, \varphi'_2)
\end{aligned}
$$

such that:

$$
\begin{aligned}
\varphi_1' &= \varphi_1 + I_1 \\
\varphi_2' &= \varphi_2 - I_2 + mI_2^2 \\
I_1' &= I_1 - \varepsilon \frac{\sin \varphi_1'}{(\cos \varphi_1' + \cos \varphi_2' + c)^2} \\
I_2' &= I_2 - \varepsilon \frac{\sin \varphi_2'}{(\cos \varphi_1' + \cos \varphi_2' + c)^2}.
\end{aligned}
\tag{7}
$$

where (I, φ) are the action-angle variables $(I, \varphi) \subseteq \mathbb{D} \times \mathbb{T}^n$ with $\mathbb{D} \subseteq \mathbb{R}^n$ open and bounded. In addition to the perturbing parameter ε, the map contains a parameter m which regulates the intensity of steepness.

We remind that the above map corresponds to the 1-time flow of the Hamiltonian whose unperturbed part is:

$$
h(I_1, I_2, I_3) = \frac{I_1^2}{2} - \frac{I_2^2}{2} + m\frac{I_2^3}{3} + 2\pi I_3 \tag{8}
$$

and the perturbing function is:

$$
f = \frac{1}{\cos \varphi_1 + \cos \varphi_2 + c} \tag{9}
$$

and has a full Fourier spectrum. The application of the Nekhoroshev theorem to symplectic maps was illustrated in Guzzo (2004).

In the following, we verify the convexity, quasi-convexity and 3-jet condition for the Hamiltonian (8).

i) *The convexity* of the Hamiltonian (8) we check by inserting this function into the equation (4) that becomes:

$$
u_1^2 - (1 - 2mI_2)u_2^2 = 0 \tag{10}
$$

and has trivial solutions only for

$$
1 - 2mI_2 < 0 \Leftrightarrow I_2 > \frac{1}{2m}. \tag{11}
$$

In this domain the function h is *convex*, while for $I_2 < 1/2m$ the convexity is not satisfied.

ii) The system (5) with h equal to (8) is:

$$
\begin{aligned}
u_1^2 - (1 - 2mI_2)u_2^2 &= 0 \\
I_1 u_1 + I_2(mI_2 - 1)u_2 + 2\pi I_3 u_3 &= 0
\end{aligned}
\tag{12}
$$

and has trivial solutions for $I_2 > 1/2m$ which implies quasi convexity in this domain.

iii) Finally, the three equations determining the *3-jet condition* for the Hamiltonian (8) are:

$$
\begin{aligned}
u_1^2 - (1 - 2mI_2)u_2^2 &= 0 \\
I_1 u_1 + I_2(mI_2 - 1)u_2 + 2\pi I_3 u_3 &= 0 \\
2mu_2^3 &= 0.
\end{aligned}
\tag{13}
$$

When $m = 0$ the system has non trivial solutions in all the three cases, i.e. it does not satisfy any of the three classes of steepness. For $m \neq 0$ the system has trivial solutions only and it satisfies the $3 - jet$ condition.

It is easy to control the intensity of steepness by a simple variation of the steepness parameter m. With a parameter that directly acts on the steepness properties, the map (7) is a promising candidate for experiments we would like to perform. We are interested to observe the influence of the steepness parameter on the dynamics in the non convex ($I_2 < 1/2m$) steep ($m \neq 0$) domain of the model.

4. THE ARNOLD WEB OF THE MODEL

The Arnold web is a peculiar low measure set of quasi integrable non degenerate systems nested in the dense set of KAM tori. While the initial conditions taken on KAM tori are stable at infinite times, the Arnold web is the source of instabilities in the system. The pioneering work on this topic was done by Arnold (Arnold 1964) who used a simple Hamiltonian to illustrate a "mechanism for instability" with the possibility for a drift of actions along a resonance. Following this description the term *Arnold diffusion* is a name for related phenomena. Even though the exact analytical description of such motions still does not exist, a large amount of numerical research is done confirming the possibility for the Arnold-like diffusion along a resonance in many dynamical models, mainly given by symplectic maps (Froeschlé et al. 2005, Guzzo et al. 2005, Guzzo et al. 2006, Todorović et al. 2008, Guzzo et al. 2009, Guzzo et al. 2011).

The projection of the Arnold web on the frequency space satisfies the so called resonance condition:

$$
\sum k_i \omega_i = 0, \quad i = 1, ..., n. \tag{14}
$$

Applied to the Hamiltonian (8) the above equation gives the generic form of resonances in our model:

$$
k_1 I_1 + k_2(mI_2^2 - I_2) + 2k_3\pi = 0 \tag{15}
$$

with $k_1, k_2, k_3 \in \mathbb{Z}$. For $m \neq 0$ the set (15) corresponds to a set of parabolas, while for $m = 0$ the resonances are linear since the quadratic term in actions $k_2 mI_2^2$ coupled to the steepness parameter m disappears.

One of the most useful numerical tools used to obtain the structure of the Arnold web is the fast Lyapunov indicator- FLI (Froeschlé et al. 1997, Froeschlé et al. 2000, Guzzo et al. 2002). The FLI reflects the growth of a tangent vector v of a given initial vector x in a fixed time t : $FLI_t(x, v) = \log \|v_t\|$. FLI recognizes not only the ordered from chaotic motions, but it also distinguishes between regular resonant motions and motions on KAM tori. Moreover, FLI is able to make the difference between different kinds of chaotic orbits, revealing the very fine structure inside the chaotic domain composed by stable and unstable manifolds of the hyperbolic invariant manifolds (Lega et al. 2010).

27

Using the mentioned properties, with FLI it is possible to visualize the resonant structure of the model (the technique is described in Froeschlé et al. 2000). Fig. 1 shows the Arnold web of the model obtained with FLI computed for 1000 iterations on a 500×500 grid of initial actions regularly spaced on $I_1 \times I_2 = [0, \pi] \times [0, \pi]$ and for fixed initial angles $\varphi_1 = 0, \varphi_2 = 0$, and tangent vectors $(v_{I_1}, v_{I_2}, v_{\varphi_1}, v_{\varphi_2}) = (1, 1, 0.5(\sqrt{5} - 1), 1)$.

In the top three plots, the perturbation is $\varepsilon = 0.03$, the system is dominated by regular orbits marked by dark gray in the figure (red in the color version). In the lower three plots the perturbation is higher, $\varepsilon = 0.1$ and the size of the chaotic zone (light gray in the plot and yellow in the color version) considerably increases. In the two left plots $m = 0$: the system is not steep (studied in Guzzo et al. 2006). The bending of the resonances is appreciable already for $m = 0.1$ plotted on the two middle panels and becomes evident in the two right plots where the parameter of steepness is $m = 0.3$. The two middle panels show only the steep non convex domain. For $m = 0.3$ (Fig. 1, right panels) only the region below the white (yellow in the color version) dashed line $I_2 = 1/2m \sim 1.67$ is steep and non convex, while the region above the line is quasi-convex.

The presence of KAM tori in the quasi-convex region (above the dashed line) is higher than for the steep non-convex one (below the dashed line); this effect is more evident in the bottom right plot, where the system is generally more chaotic. This is in agreement with the Nekhoroshev statement of greater stability in the quasi-convex domains.
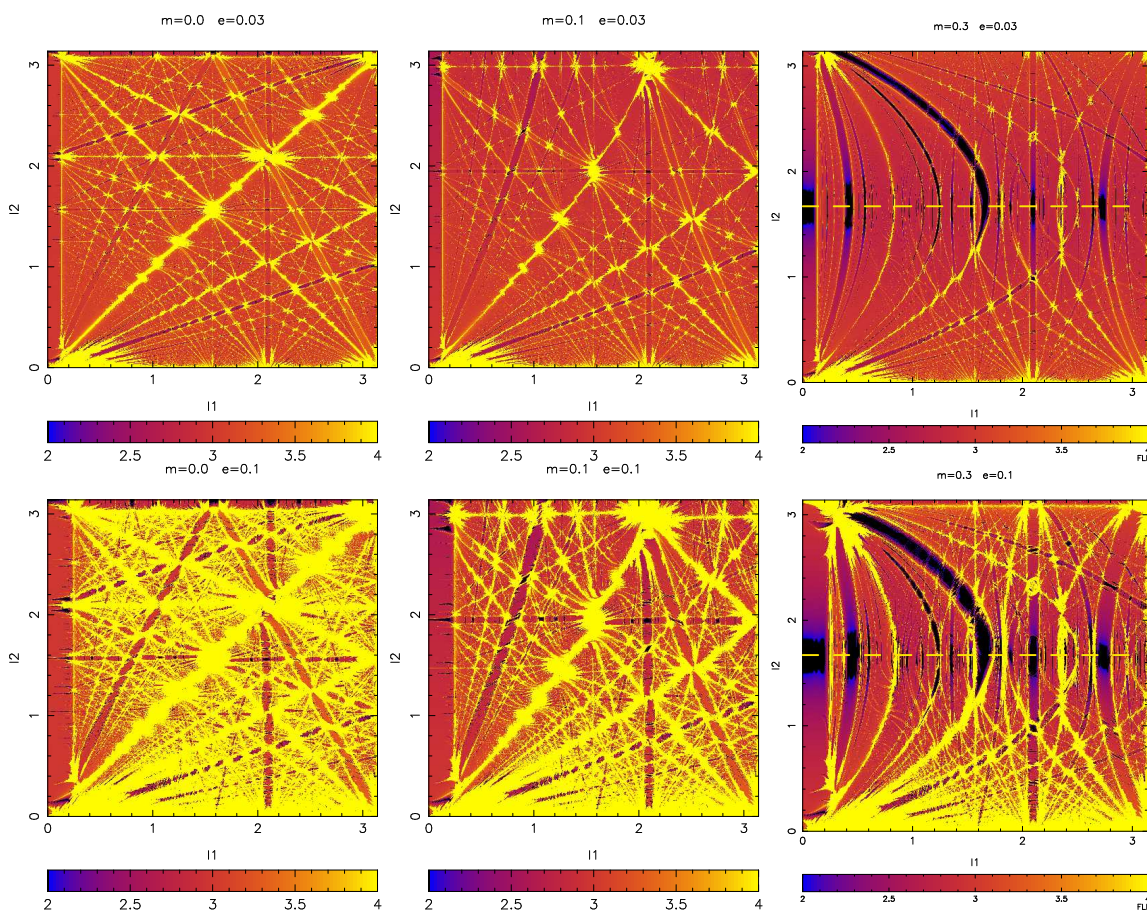

Fig. 1. *The FLI chart for the system (7) obtained with FLI computed with 1000 iterations on $(I_1, I_2) = [0, \pi] \times [0, \pi]$. The dark gray orbits represent the stable KAM tori background, while the white lines represent resonances in the set (15) reflecting the structure of the Arnold web. In the **top plots** $\varepsilon = 0.03$, the dynamics is dominated by regular orbits (dark gray). In the **bottom plots** $\varepsilon = 0.1$ and the system has more chaotic orbits (light gray). In the **left plots** $m = 0$ the system is not steep and not convex. The system is influenced by a week steepness effect with m=0.1 in the **middle two plots** and with a stronger steepness ($m = 0.3$) in the **right two plots**. In the right two plots we notice a certain difference in the stability for the steep non convex region which is below the dashed line and the quasi-convex region above the line.*

When the perturbation ε increases the number of tori decreases and resonances start to overlap according to the well known Chirikov criterion. We will call ε_c the critical value of the perturbing parameter for which the dynamics is dominated by the overlapping of resonances, i.e. the system enters the Chirikov regime. We say that the system is in a Nekhoroshev like regime when the dynamics is dominated by KAM tori, i.e. for $\varepsilon < \varepsilon_c$. We check in what follows the influence of the parameter m on this transition in order to show that ε_c depends also on the steepness parameter. In the same domain as for the Fig. 1, we count the number of chaotic orbits ($FLI > 4.5$ for 1000 iterations) and observe its change with m.

The result is plotted in Fig. 2. The three lines show the value of ε for which 50 %, 60% and 70% of orbits respectively are chaotic. The plot shows that for $m < 0.1$, the critical ε is almost constant: $\varepsilon_c \sim 0.1$. For $m \in [0.1, 0.3]$ the more stable quasi-convex region (above the dashed line in the Fig. 1 right) enters the $[0, \pi] \times [0, \pi]$ domain, which increases the critical value to $\varepsilon_c \in [0.4, 1]$. For $m > 0.3$, a low order resonance $I_2 = 1/m$ with its strong chaotic neighborhood enters the observed domain and ε_c decreases again. The experiment shows that ε_c is not affected by m for lower values of the steepness parameter. At some point, approximately at $m \sim 0.1$, the critical ε becomes significantly influenced by the steepness parameter.
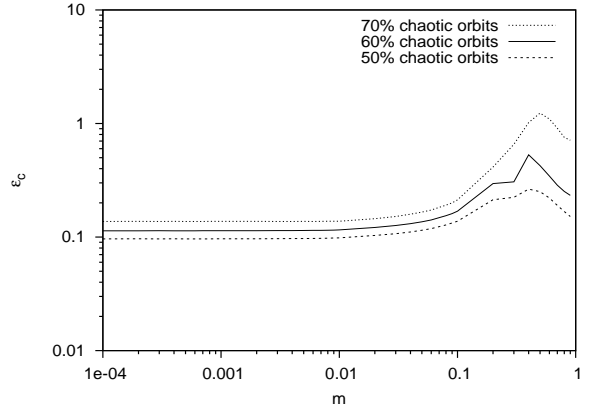

Fig. 2. *The critical ε against m for $m \in [10^{-4}, 1]$. The three lines correspond to the situations when 50%, 60% and 70% of orbits in the action domain $[0, \pi] \times [0, \pi]$, grid 500×500 are chaotic ($FLI > 4.5$ for 1000 iterations). For $m < 0.1 : \varepsilon_c \sim 0.1$. For $m \in [0.1, 0.3]$ the more stable quasi-convex domain enters into the observed region and ε_c increases. For $m > 0.3$, ε_c decreases again since a strong resonance ($I_2 = 1/m$) enters the observed domain.*
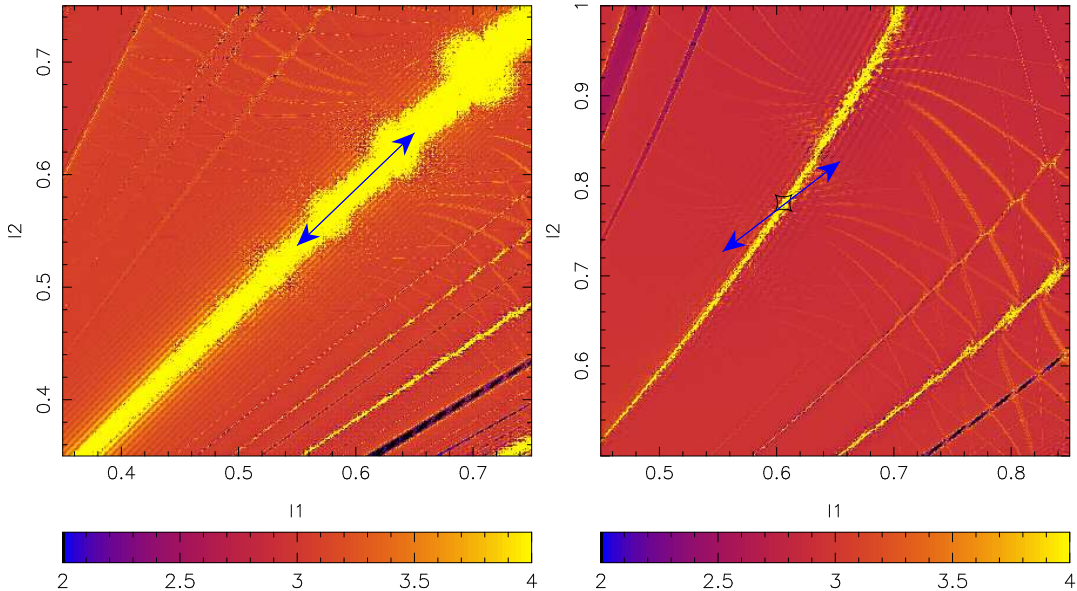

Fig. 3. *For a non convex system ($m=0$, the left panel) the fast drift line is contained in the resonance and provokes fast diffusion along it. The steepness effect bends the resonances to a parabola, while the fast drift line remains on the 1-1 direction ($m=0.3$, the right panel). This is basically a mechanism responsible for the slowing down effect of steepness. The arrow on both panels shows the direction of the fast drift line.*

29

5. DIFFUSION ALONG THE RESONANCE AND THE DIFFUSION COEFFICIENT COMPUTATION

An important role in the resonant dynamics plays the so called *fast drift line*. The position of the fast drift line with respect to the resonance affects the diffusion properties in the resonance. A detailed description of this issue can be found in Nekhoroshev (1977) and Morbidelli and Guzzo (1997). The model we study is designed in such a way that the position of the fast drift line is directly related to the steepness properties i.e. the steepness parameter m. The resonance we observe is:

$$mI_2^2 - I_2 + I_1 = 0. \qquad (16)$$

In the resonant set (15) it is the $(1,1,0)$ resonance. For the non convex case (when $m = 0$) this resonance belongs to a web of resonances such that its fast drift line is contained in the resonance, which provokes fast diffusion along it. This situation is plotted in the left panel of the Fig. 3 where the arrow represents the fast drift line. The fast diffusion along the resonance (16) for this case was observed and studied by Guzzo et al. (2006). As the parameter m increases, the resonance becomes parabolic, while the fast drift line remains on the $1 - 1$ direction. Their mutual collinearity is lost which slows down the diffusion. In the right panel of the Fig. 3 there is a segment of the FLI chart with the same resonance and its fast drift line (marked with an arrow which lies out of the resonance on the 1-1 direction) when the system is steep, for $m = 0.3$. The diffusion along the resonance in this situation is significantly slower than for the non convex case.

The computation of the diffusion coefficient

As already mentioned, the motion in the resonance does not have an analytical solution. We provide estimates on its dynamics statistically, treating it as a Brownian type motion. The algorithm we use to compute the diffusion coefficient is taken from Lega et al. (2003) and Froeschlé et al. (2005).

For a set of N initial actions $(I_1^j(0), I_2^j(0))$ and $\varphi_{1,2}^j = 0$ with $j = 1, N$ properly chosen $(FLI(I) > 1.5 \log t)$ on the resonance (16) the map is iterated 10^k times. The diffusion coefficient is defined as the mean square linear increase of actions with respect to their initial values. Numerically, it is the best linear fit of the quantity:

$$S_1(t) = \frac{1}{N} \sum_{j=1,N} (I_2^j(t) - I_2^j(0))^2 + (I_1^j(t) - I_1^j(0))^2 \qquad (17)$$

where $(I_1^j(t), I_2^j(t))$ are the actions after the iteration time t.

An alternative way, more convenient from the numerical point of view is to observe only the restriction of the motion to the plain s given by:

$$s = \{(I_1, I_2, \varphi_1, \varphi_2) : (\varphi_1, \varphi_2) = (0,0)\}.$$

Again, the diffusion coefficient D is defined as the best linear fit of the mean square linear increase of the diffusing orbits with respect to their initial values, taking into account only their crossings with the plain s i.e. it is the coefficient of the regression line fitted through:

$$S_2(n\Delta t) = $$
$$= \frac{1}{M_n} \sum_{i:|\varphi_1^i + \varphi_2^i| < \delta} (I_2(t) - I_2(0))^2 + (I_1(t) - I_1(0))^2. \qquad (18)$$

The total iteration time t is divided into a certain number of subintervals Δt. M_n is the number of orbits which cross the plain s during the n-th interval i.e. satisfy the condition $|\varphi_1^i + \varphi_2^i| < \delta$. The crossing of the orbit (I_1^i, I_2^i) and the plain s actually corresponds to the condition $(\varphi_1^i, \varphi_2^i) = (0,0)$. Due to numerical reasons, this condition is weakened and we observe the crossings of the orbits with the δ slices of the plain s. The size of the slices is chosen according to the number of initial orbits and iteration times.

The two ways to compute the diffusion coefficient reflect the same phenomena and should give approximately the same values of the diffusion coefficient. We denote with D_{EI} the diffusion coefficient computed from the quantity $S_1(t)$ and by D_{IP} the one obtained from $S_2(n\Delta t)$. Fig. 4. shows one example where the two ways of the diffusion coefficient computation show a good agreement. The upper line
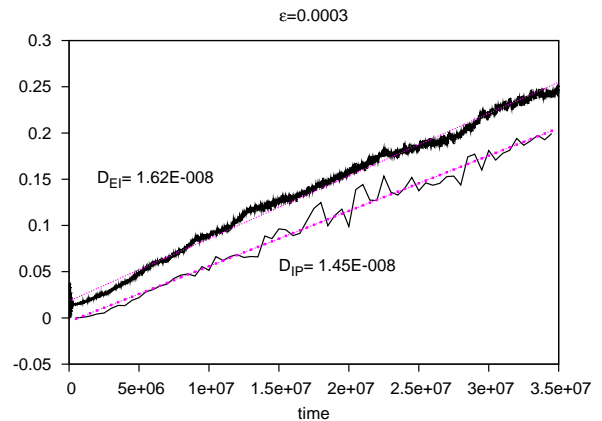

Fig. 4. *The top curve represents the change of the quantity $S_1(t)$ giving the diffusion coefficient $D_{EI} = 1.62 \times 10^{-8}$. A close value $D_{IP} = 1.45 \times 10^{-8}$ shows the lower $S_2(n\Delta t)$ line where only the intersection points of the diffusing orbits and the action plain are considered (the parameters for this plot are $m = 0.001$ and $\varepsilon = 0.0003$).*

shows the quantity $S_1(t)$ and the corresponding diffusion coefficient $D_{EI} = 1.62 \times 10^{-8}$. The lower line shows the change of the quantity $S_2(n\Delta t)$ in time and gives a very close value for the diffusion coefficient $D_{IP} = 1.45 \times 10^{-8}$. The parameters are $m = 0.001$, $\varepsilon = 0.0003$ and iteration time is $t = 3.5 \times 10^7$.

6. THE RESULTS ON DIFFUSION

It is very difficult to confirm numerically the exponential stability provided by the Nekhoroshev theorem. Even more difficult would be to observe *the change* of those exponential laws as the steepness effect increases. The numerically obtained relation between the diffusion coefficient D and ε usually covers a small interval in ε which is not trustful for a good exponential fit. In previous works on the Nekhoroshev stability (Guzzo et al. 2005, Guzzo et al. 2006, Todorović et al. 2008) this dependence was usually fitted by two or more power laws, which increase as the perturbation decreases. This results is interpreted as a strong indication for an exponen-

tial dependence. In order to recover the expected changes in the diffusion speed with steepness, we observe the relation between the diffusion coefficient D and the size of the perturbation ε for five different values of the steepness parameter m. We expect to observe the increase of the power laws with growth of the parameter m.

The choice of the initial conditions to compute diffusion should be carried out carefully. We choose a set of N initial conditions in the close neighborhood of the point (I_1^0, I_2^0). The value $I_1^0 = \omega_1$ is taken as a strong irrational number $\omega_1 = \pi/3\sqrt{3} \sim 0.604$ [1]. The corresponding action I_2^0 lying on the resonance (16) is $I_2^0 = (1 - \sqrt{1 - 4m\omega_1})/2m$. In this computation, the number of initial orbits N goes from 200 for the slower diffusion up to 1000 for fast diffusing orbits. The iteration times range from 10^5 up to 10^{10}.

The results of the computation are presented in Fig. 5. The plot shows the change of $\log_{10}\varepsilon$ against $\log_{10}D$ for five different values of the parameter $m = \{0.001, 0.01, 0.03, 0.1, 0.3\}$. For the lowest steepness parameter $m = 0.001$ we computed 16 values of the diffusion coefficient in the interval $\varepsilon \in [9 \times 10^{-6}, 5 \times 10^{-4}]$ with two fitted power laws
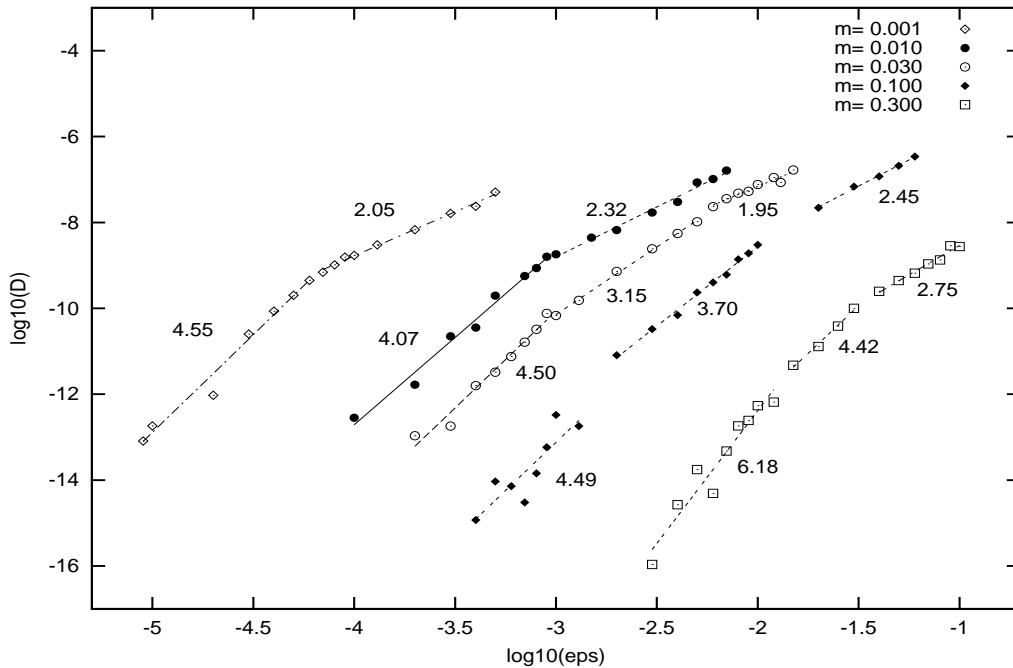

Fig. 5. *The change of the diffusion coefficient D against the perturbation ε for five different values of the steepness parameter $m = \{0.001, 0.01, 0.03, 0.1, 0.3\}$. For every data set (every fixed m) the plot shows a broken power law which indicates an exponential dependence. Increasing the steepness effect should increase the values of the fitted power laws. Each of the plotted data sets corresponds to another interval of ε which prevents their direct comparison. Taking into account that the power laws increase as the perturbation decreases, the computed results give an indirect confirmation of the expected result.*

---

[1] Being close to a rational frequency value means close to another resonance. The orbits could eventually diffuse along it which would give a wrong result on the diffusion coefficient along the resonance we study.

4.55 and 2.05. For $m = 0.01$ again 16 values of the diffusion coefficient are computed in the interval $\varepsilon \in [10^{-4}, 0.007]$ with two power laws 4.07 and 2.32. The third data set in the plot corresponds to the steepness parameter fixed on $m = 0.03$ where 22 values of D are computed in the interval $\varepsilon \in [2 \times 10^{-4}, 0.015]$. The three fitted power laws are 4.50, 3.15 and 1.95. For the steepness parameter $m = 0.1$ another 22 values of the diffusion coefficient are computed in the interval $\varepsilon \in [6 \times 10^{-4}, 0.05]$ with three power laws 4.49, 3.70 and 2.45. Along the line that corresponds to the power 4.49 we notice a significant variation around the fitted line which may suggest oscillations in D for lower values of ε. The possibility that this oscillation is a consequence of the numerical instabilities is also not excluded. Finally, for the highest observed steepness effect with $m = 0.3$ we computed 20 values of the diffusion coefficient in $\varepsilon \in [1 \times 10^{-3}, 0.1]$. Three power laws: 6.18 , 4.42 and 2.75 are fitted through this data set. Again a certain oscillation around the fit 6.18 can be noticed.

For every observed data set we obtain very similar values of the power laws (around 2, 4 and only one close to 6), which gives the impression that they remain constant, opposite to our expectations. Taking into account that for every m we observe different intervals in ε (the intervals in ε shift to higher values as m increases) the power laws for different m can not be directly compared. The reason we are limited in the ε intervals are only numerical. On the other hand, we already mentioned that the power laws increase as the perturbation decreases.

This leads to the conclusion that the expected increase of the power functions with m is present-but is not *directly* observable. In this way our expectations on the stabilizing steepness effect are indirectly confirmed.

7. CONCLUSIONS

The change of the resonant structure, stability and the diffusion laws as a consequence of the increasing steepness effect is observed. The experiment is performed on a 4-dimensional steep symplectic map using methods developed in the last decade. The resonant structure and the global stability evidently change as the effect of steepness increases. The obtained results on the diffusion laws, although limited numerically, give a strong indication that steepness plays a significant role in the change of the diffusion speed.

REFERENCES

Arnold, V. I.: 1964, *Sov. Math. Doklady*, **5**, 342.
Celletti, A. and Giorgilli, A.: 1991, *Celest. Mech. Dyn. Astr.*, **50**, 31.
Efthymiopoulos, C.: 2005, *Celest. Mech. Dyn. Astr.*, **92**, 29.
Froeschlé, Cl., Gonczi, R. and Lega, E.: 1997, *Planetary and Space Science*, **45**, 881.
Froeschlé, C. and Lega, E.: 2000, *Celest. Mech. Dyn. Astr.*, **78**, 167.
Froeschlé, C., Guzzo, M. and Lega, E.: 2000, *Science*, **289**, 5487.
Froeschlé, C., Guzzo, M. and Lega, E.: 2005, *Celest. Mech. Dyn. Astr.*, **92**, 243.
Giorgilli, A. and Skokos, C.: 1997, *Astron. Astrophys.*, **317**, 254.
Guzzo, M., Lega, E. and Froschlé, C.: 2002, *Physica D*, **163**, 1.
Guzzo, M.: 2004, *Annales Henry Poincare*, **5**, 1013.
Guzzo, M., Lega, E. and Froschlé, C.: 2005, *DCDS B* **5**, 3.
Guzzo, M., Lega, E., and Froeschlé, C.: 2006, *Nonlinearity*, **19**, 1049.
Guzzo, M. and Morbidelli, A.: 1996, *Celest. Mech. Dyn. Astr.*, **66**, 255.
Guzzo, M., Knežević, Z. and Milani, A.: 2002, *Celest. Mech. Dyn. Astr.*, **83**, 121.
Guzzo, M., Lega, E. and Froeschle, C.: 2011, *Chaos*, accepted.
Lega, E., Guzzo, M. and Froeschlé, C.: 2003, *Physica D*, **182**, 179.
Lega, E., Guzzo, M. and Froeschl, C.: 2010, *Celest. Mech. Dyn. Astr.*, **107**, 115.
Lhotka, Ch., Efthymiopoulos, C. and Dvorak, R.: 2008, *Mon. Not. R. Astron. Soc.*, **384**, 1165.
Morbidelli, A. and Guzzo, M.: 1997, *Celest. Mech. Dyn. Astr.*, **65**, 107.
Nekhoroshev, N. N.: 1977, *Russ. Math. Surv.*, **32**, 1.
Pavlović, R. and Guzzo, M.: 2008, *Mon. Not. R. Astron. Soc.*, **384**, 1575.
Todorović, N. Lega, E. and Froeschlé, C.: 2008, *Celest. Mech. Dyn. Astr.*, **102**, 13.
Todorović, N. Guzzo, M. Lega, E. and Froeschlé, C.: 2011, *Celest. Mech. Dyn. Astr.*, in press (DOI: 10.1007/s10569-011-9369-8).

УТИЦАЈ ПАРАМЕТРА СТРМОСТИ НА ЕКСПОНЕНЦИЈАЛНУ СТАБИЛНОСТ У МОДЕЛУ ПРОСТОРА. НУМЕРИЧКИ АСПЕКТИ

N. Todorović

Astronomical Observatory, Volgina 7, 11060 Belgrade 38, Serbia

E–mail: *ntodorovic@aob.rs*

Нехорошевљева теорема несумњиво спада у једно од најзначајнијих достигнућа модерне небеске механике. Уз хипотезу да је хамилтонијанска функција аналитичка, да је њен интеграбилни део недегенеративан тј. да задовољава математички услов стрмости, теорема обезбеђује стабилност акција у експоненцијално дугом временском интервалу. Такође, Нехорошев је у свом раду из 1977. наговестио да би повећање стрмости имало за последицу и већу стабилност акција. Помоћу нумеричких метода које су развијене у последњој децениjи, ова претпоставка је верификована. Коришћен је модел 4-димензионе симплектичке мапе која задовољава хипотезе Нехорошевљеве теореме и која поред поремећајног параметра ε, садржи и параметар m којим се директно регулише интензитет стрмости. За пет различитих вредности параметра стрмости m нумерички је мерена зависност између брзине дифузије D дуж одабране резонанце и поремећајног параметра ε. Добијени резултати указују на то да се степен функције која је фитована кроз добијене резултате повећава са повећањем параметра стрмости, те је на тај начин Нехорошевљева претпоставка нумерички потврђена.